Coastal Dynamics 2017
Paper No. 137

FLASH RIP STATISTICS FROM VIDEO IMAGES

Guy Rodier Mabiala[1], France Floc'h[2], Rafaël Almar[3], Bruno Castelle[4], Nicholas Halls[3], Yves Du Penhoat[13] and Tim Scott[5]

Abstract

The coastal area of the Gulf of Guinea is vulnerable to the phenomenon of coastal erosion. Many authors already proved that rip currents play a crucial role in coastal morphodynamic and erosion processes. The coexistence of Swash and Flash rip-currents at Grand-Popo beach was shown using lagrangian buoys measurements. In order to study the hydrodynamic conditions related to the generation of flash rip currents, a method based on color processing of the video image has been set up to detect the presence of rip-currents via a change of turbidity, to extract their characteristics and to study their link with forcings. During our study, 434 events of the rip-currents were counted over one short period of 7 days. The majority of rips occurs at low tide as already mentioned in literature, migrates down-drift. Flash rip activity was maximized for shore-normal wave incidence and significant wave height of 1.2-1.5 m.

Key words: hydrodynamics; Flash-rip; video imaging; Grand-Popo beach; erosion; coastal.

1. Introduction

RIP currents are cross-shore coastal currents. They are narrow and oriented offshore with high speeds (about a m/s) and often appear along steep sandy beaches dominated by waves (or swells). According to the review of Castelle et al. (2016), they are now classified in three main types: focused, fixed, and flash rips. Focused and fixed rips are coupled with three-dimensional bathymetric features and forced by hard structures in the surf zone, respectively, while flash rips are generated by transient nearshore flow instabilities. The focused and fixed rips are quite well described in the literature while flash rips are poorly documented. The majority of authors converge towards two principal mechanisms based respectively on shearing instabilities of the longshore current and the horizontal vorticity induced by the wave breaking spatial variations. The forcing terms in linear wave theory are defined as the radiation stress by Longuet-Higgins and Stewart (1964).

Rip-currents are an important mechanism for the cross-shore exchange of water, nutrient, larvae, pollutant and sediment between the surf zone and the upper shelf (Shanks et al, 2010). These currents also contribute to sediment transport (Cooke, 1970; Komar, 1971; Shorts, 1999) often in great quantity (Brander R.W, 1999; Inman D. and al., 1971). They thus play a crucial role in coastal morphodynamic and erosion processes (Shorts, 1992) especially during storms (Thornton and al., 2007; Birrien and al., 2013). These currents represent the principal death hasard by drowning, for beach users around the world. It has been reported that the African area has the highest drowning rate in the world (Peden and McGee, 2003; WHO, 2010). However the occurrence and the type of rip developing on African beaches remains poorly documented. Using Lagrangian drifters released in the surf zone, Castelle and al. (2013) has shown the coexistence of swash and flash rips on the beach of Grand-popo. Since the flash rips are transitory in time and space, field data on their dynamics is sparse, and video-imaging appears to be a suitable approach to capture their dynamics on large temporal and space scales. But the few direct observations of this kind of current, on the Gold Coast in Australia, revealed a low probability of capture (0, 52%) over a single period of observation (Murray and al., 2013). Since most of world littorals, The coastal area of the Gulf of Guinea

[1] CIPMA & IRHOB, Cotonou, Bénin - m.guyrodier@yahoo.fr ; yves.du-penhoat@ird.fr
[2] Domaines Océaniques UMR6538/UBO/IUEM, 29280 Plouzané, France – france.floch@univ-brest.fr
[3] IRD-LEGOS (CNRS/IRD/CNES/UPS) 31400 Toulouse, France – rafael.almar@ird.fr ; nick.hall@legos.obs-mip.fr
[4]CNRS/Unv. Bordeaux, UMR EPOC, Allée Geoffroy Saint-Hilaire, France - bruno.castelle @ u-bordeaux.fr
[5] University of Plymouth, Drake Circus, Plymouth, PL4 8AA, UK - timothy.scott@plymouth.ac.uk

is vulnerable to the phenomenon of coastal erosion. With a view to understand the hydrodynamic process related to the generation of flash rip currents, we set up a method based on image processing in order to detect the presence of rip-currents according to the surface turbidity, to extract their characteristics and to study their link with hydrodynamic forcings. The general objective is to analyze the hydrodynamic conditions related to the generation of flash rip currents.

2. METHODS

2.1. *Study site*

Grand Popo is an open wave-dominated and microtidal beach (mean spring tide range:~1.8 m) exposed to long period swells with a mean significant wave height $Hs = 1.36m$ and a mean peak wave period $T_P = 9.4s$. The combination of the medium to coarse quartz sand ($0.4–1mm$, $D50: 0.6\,mm$) and dominant groundswell regime generated in the South Atlantic results in a modal intermediate, somewhat reflective, beach state corresponding to the low-tide terrace state following Wright & Short (1984). The combined effect of persistent swells throughout the year and beach steepness results in an intense easterly longshore drift of about $0.8 \times 10^6\ m^3/year$ (Laïbi et al., 2013). During the 10-day field campaign, the wave and tide conditions are obtained from an ADCP moored in 12m of depth, beyond the surf zone. Video footage were acquired at $2Hz$, from a video system mounted on a 15 m-high tower, located at about $80m$ from the mean waterline.

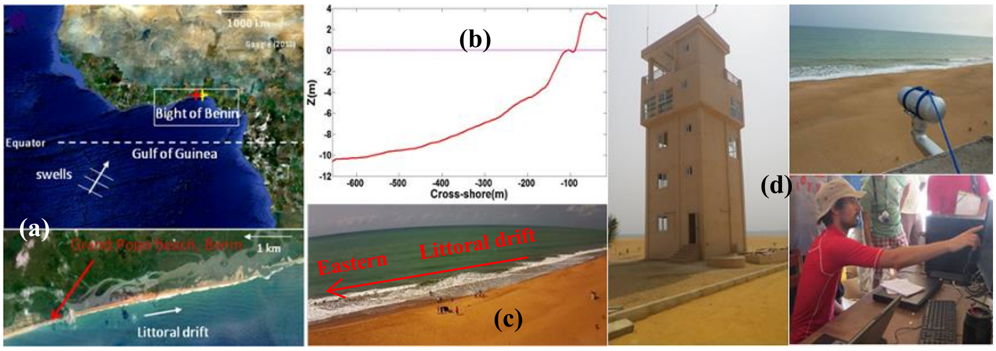

Figure 1: *(a)* Location of the Grand Popo beach; *(b)* Vertical profile of beach; *(c)* field of study; *(d)* tower and video system.

2.2. *Experimental Methods*

2.2.1. *Images rectification*

A orthocorrection was applied to the images in order to see a projection of the image in a horizontal plan. This correction consists on:

- cutting out (Figure 2.a) on each instantaneous image the zone of interest of better pixel resolution following the longshore direction and including the surf and swash zone;
- correcting the image distortion due to the lens;
- georeferencing the images, according to the ground control point of Grand-Popo taken with a DGPS-RTK (Origin: foot of the semaphore).

The final image obtained presents a plan view of the site and informs us directly about the real positions compared to the ground control point of the study (Figure 2 b).

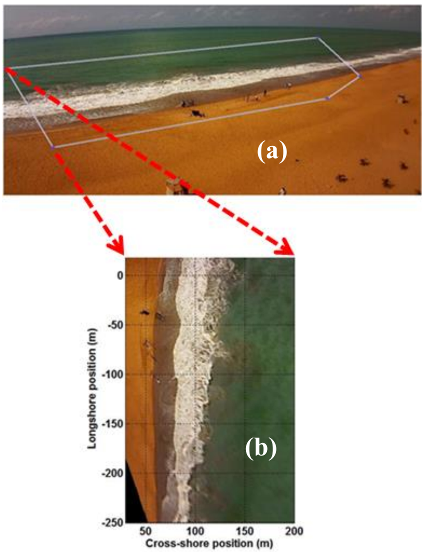

Figure 2: *(a)* Interest zone determination ; *(b)* Rectified and georeferenced image.

Over seven days of video measurement (March 12th-18th, 2014), after quality control, considering only the clearest daylight hours (from 8:00 to 16:00), 57 hours of images has been processed.

2.2.2. *Image processing*

The detection of rip-currents on the rectified instantaneous images is a very long task if done manually image by image. This is due to the quantity of images (57 × 60 × 120 = 410400 images) to visualize. Thus an automatic method has been developed and set up, based on color processing of images. As the flash rip-currents transport a large amount of sediments in suspension offshore beyond the surf zone, the surface water is browner within the rip than in the surrounding sea (which is greener). Detection of rip-currents is thus based on treatment of the colors of images: initially a threshold on the red in RGB format is used to remove the part of beach and swash zone in the image. In order to reinforce the contrast between green and brown outside the surf zone, a threshold on color in HSV-format is applied (Figure 3.c).

The automatic detection of flash rip-currents is carried out on a longshore time-stack (Figure 3.b), over 10 minutes in format HSV, starting from the rectified images. In order to detect the flash rip at different positions during its lifetme, four stacks were positioned in parallel (Figure 3a). Once detected, a visual control was done to confirm the presence of a flash rip current. Then morphology characteristics of the flash rip were computed from a set of instantaneous images (from the beginning to the end of detection, the complete estimated lifetime of the flash-rip).

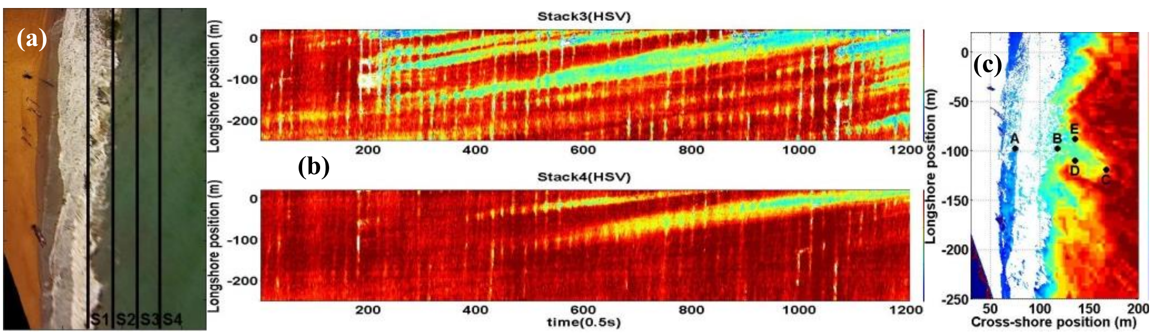

Figure 3: (*a*) Initial image with long-shore stacks positions; (*b)* Example of long-shore time-stacks showing rip current *(c)* Processed image with five characteristics points.

The computed characteristics are their positions (cross-shore and longshore position of the feet and the head, at the beginning and at the end), their extensions (cross-shore and longshore extension) and their migrations longshore in time, according to the detection of the 5 points (A, B, C, D and E) illustrated on figure 3 (c).

$\boldsymbol{A}$ corresponds to the waterline in front of the detected flash-rip. $\boldsymbol{B}$ is the first point where the turbidity flume is detected, on the breaking line. $\boldsymbol{C}$ is the most offshore point of the rip head and $\boldsymbol{E}$ and $\boldsymbol{D}$ define the longshore extension of the rip head. Then the beginning position (cross-shore ; longshore) is: $(\boldsymbol{X_A};\ \boldsymbol{Y_A})$; the cross-shore extension is $\boldsymbol{X_C} - \boldsymbol{X_A}$ and the longshore extension is $\boldsymbol{Y_E} - \boldsymbol{Y_D}$.

The precision of the position corresponds to the resolution in real coordinates ($0.5\ m$). The precision of the lifetime corresponds to the capture frequency (0.5 s). However, the uncertainties might be higher because of the uncertainties in the visual detection of the brown shape of the rip, not validated by current measurement, and thus difficult to estimate. Detection is sometimes impossible because of sunshine on some images leading to a white sea surface.

The mean migration velocity is calculated from the longshore migration of the head and the lifetime. The occurrence of flash rip during daylight is then correlated with the forcing parameters: waves and tide.

2.2.3. *Hydrodynamic parameters*

The directional waves spectra as well as the associated averaged parameters (significant wave height Hs, peak period Tp, peak direction Dir) were calculated from the orbital velocities measured by the four beams of an ADCP located 800 m offshore the beach, on 20 minutes burst of acquisition each hour. Hs corresponds to the significant height of the waves defined as the average of the distances peak-hollow of the third of the highest waves, the significant height of the component swells (Hs_swell) is calculated from the spectrum for frequencies going from 0.04 Hz to 0.1 Hz and the significant height of the component wind sea (Hs_wind), for frequencies higher than 0.1 Hz. Direction is represented in the following by the incidence according to the cross-shore normal of the beach. The angle between the true North and the cross-shore direction (oriented offshore) is 172°. Thus waves with normal incidence (incidence of 0°) corresponds to a wave direction of 172°. SW waves have positive incidence and SE waves have a negative incidence.

The directional spreading of wave energy is defined as the standard deviation, in radians, of the spectral width in the limit of a narrow spectrum (Kuik et al., 1988):

$$\boldsymbol{\sigma_\theta(f) = 2\left[2\left(1 - \sqrt{a_1^2(f) + b_1^2(f)}\right)\right]^{1/2}} \tag{1.1}$$

With

$$\boldsymbol{a_1(f) = \frac{\int_0^{2\pi} \cos\theta E(f,\theta)\, d\theta}{\int_0^{2\pi} E(f,\theta)\, d\theta}} \ ; \tag{1.2}$$

$$\boldsymbol{b_1(f) = \frac{\int_0^{2\pi} \cos\theta E(f,\theta)\, d\theta}{\int_0^{2\pi} E(f,\theta)\, d\theta}} \ ; \tag{1.3}$$

Where $\boldsymbol{\theta}$ = wave direction ; $\boldsymbol{f}$ = wave frequency ; $\boldsymbol{E}$ = Wave spectral energy density (frequency-directional wave spectrum) ; $\boldsymbol{a_1} et\ \boldsymbol{b_1}$ = terms of low-order Fourier moments of the frequency-directional wave spectrum. The mean wave direction at frequency $\boldsymbol{f}$ is,

$$\boldsymbol{\theta_m(f) = arctan(a_1(f)/b_1(f))}\ . \tag{1.4}$$

3. Results and Discussion

The waves and tide conditions, during the observations leading to our results, were very varied. Shifting from a neap tide (0.45-m range) to a spring tide (1.2-m range) cycle, Grand Popo beach was exposed to a waves regime of average incidence SW with an average significant wave height of 1.42 m and an average peak wave period of 10.6 s (Figure 4).

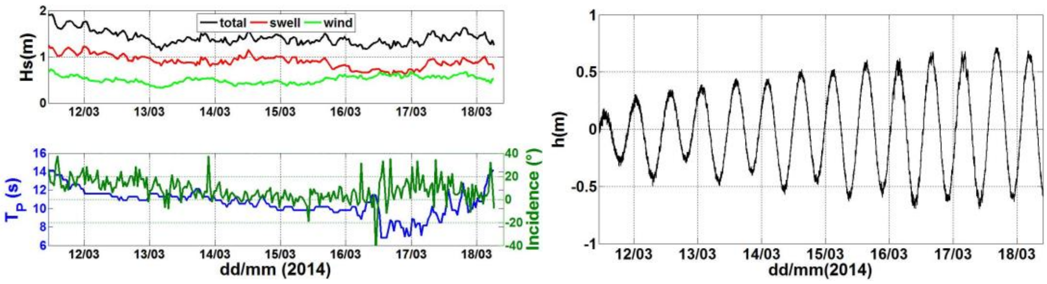

Figure 4: *(Left)* Wave conditions. *(Right)* Tide conditions.

3.1. *Qualitative Description of Flash Rip*

Several flash rip-currents have been observed on the images and their flow was characterized by a water plume charged with sediments, and turbulent sparkling water moving offshore (figure 5). The majority of the flash rip-currents has the morphology often described in the literature (MacMahan et al., 2005), with a head in the form of a mushroom, or stretched (Figure 5), and a narrow collar connecting the head to the forcing currents.

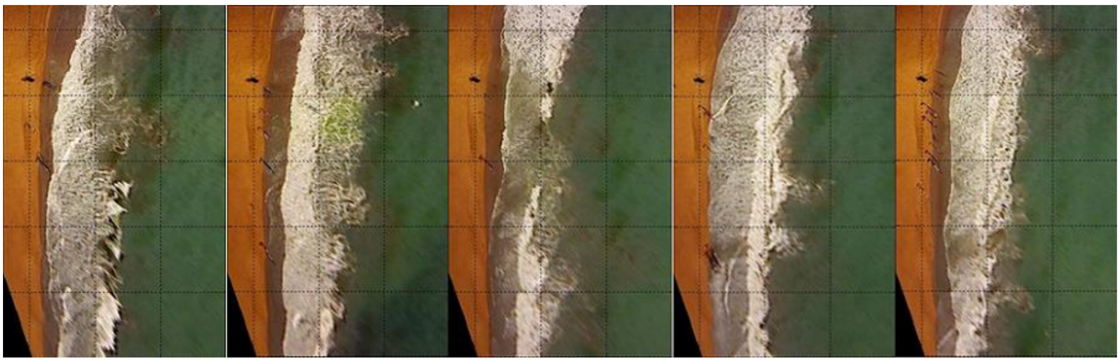

Figure 5: Morphology of rip-current (Rectified image).

3.2. *Flash rip statistics*

434 rip currents have been identified during daylight over seven days processed (57 hours video footage). This result represents a considerable extension on the work of Murray (2013) on the Gold Coast beach in Australia. However this number corresponds well the energy behavior of Grand-Popo beach, which is representative of a lot of beaches in West Africa, already noted by Castelle et al (2013). Some statistics are shown on Figure 6. Not surprisingly, the majority of the rips migrates down-drift, 60% of the rips had a lifetime between 30 and 120s (Figure 6, *Left bottom*) with 90% having a cross-shore extension between 50 and 90 m (min 35 m and max 132 m with 2 m of uncertainties; Figure 6, *Right up*). 65% of the total rips were observed to migrate alongshore with a velocity between 0.2 and 0.6 m/s (with a mean value of 0.45 m/s).
These results are in agreement with the interspersed drifter observations in Castelle et al. (2013) on the same beach and with Murray et al. (2013) in a different wave-dominated environment.

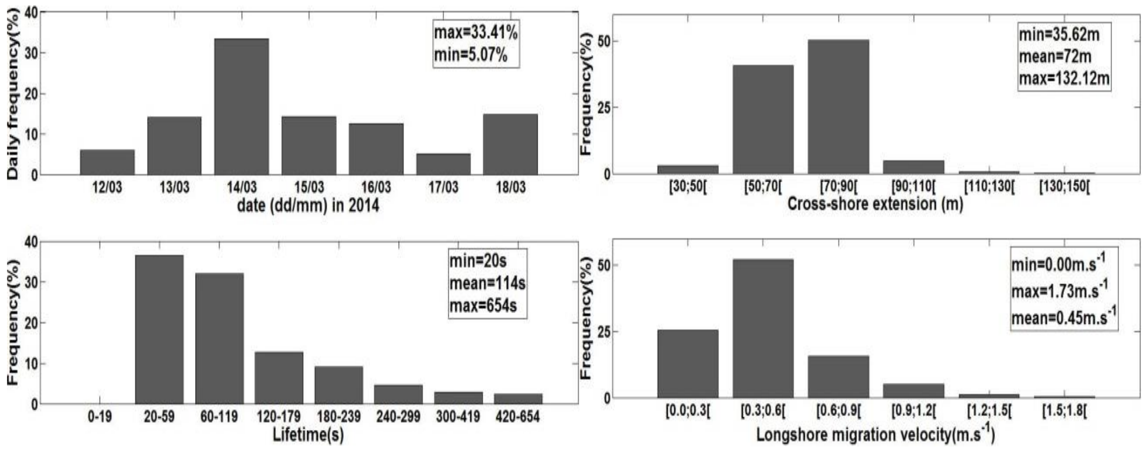

Figure 6: *(Left)* From up to bottom: Daily Flash rip statistics per day calculated over the 434 flash-rip currents detected; lifetime. *(Right)* From up to bottom: cross-shore extension; longshore migration velocity.

3.3. ***Rip Occurrence and Hydrodynamic parameters***

3.3.1. *Flash-rip vs Tide conditions*

As already shown for other rip current types (Castelle et al., 2016) maximum flash rip activity occurs at low tide (Figure 7).

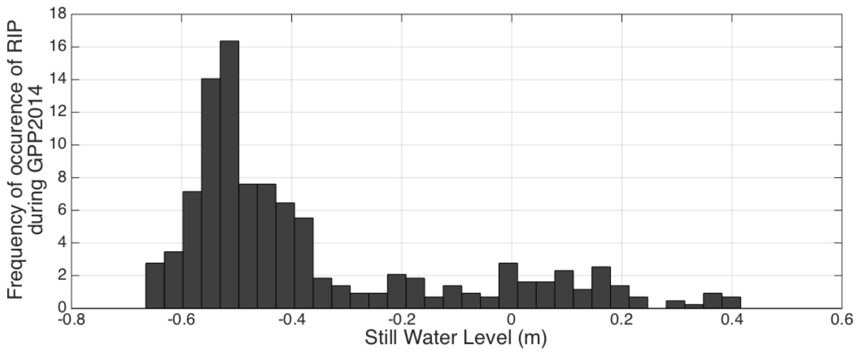

Figure 7: Frequency (%) of Flash-rip occurrence vs. Still water level.

Figure 8 represents the occurrence of flash rip-currents in time on the variation of the still water level. The dashed line (- -) indicates the hours outside the period of observation (night or too shiny). In general, the occurrence is strong for low tides and first half of flow, except for the March 12th and 13th when there is a lot of flash-RIP activity after mid-flow.

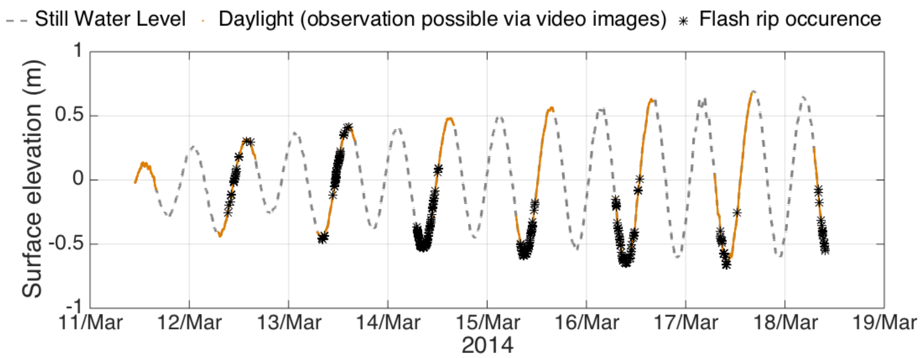

Figure 8: Temporal evolution of the Flash-rip occurrence by tidal stage.

This could be due to the influence of other environmental factors, for example the presence of an offshore wind that would support plunging breaking, by delaying the rupture of stability of the crest (Rafael Almar), which is essential in the mechanism of generation of the flash-rip (Murray, 2013).

3.3.2. *Flash-rip vs Waves conditions*

At Grand Popo, the maximum flash rip activity was observed for significant wave heights ranging from approximately 1.2 – 1.5 m (Figure 9) and peak period between 10 and 12 s. Under high energy conditions, strong turbulence is observed on the images between the breaking line and the swash zone, with no generation of flash rip-currents. These observations could be explained by the presence under such conditions of a strong onshore current, due to the Stokes drift, that tends to slow down the generation of the rip-currents.

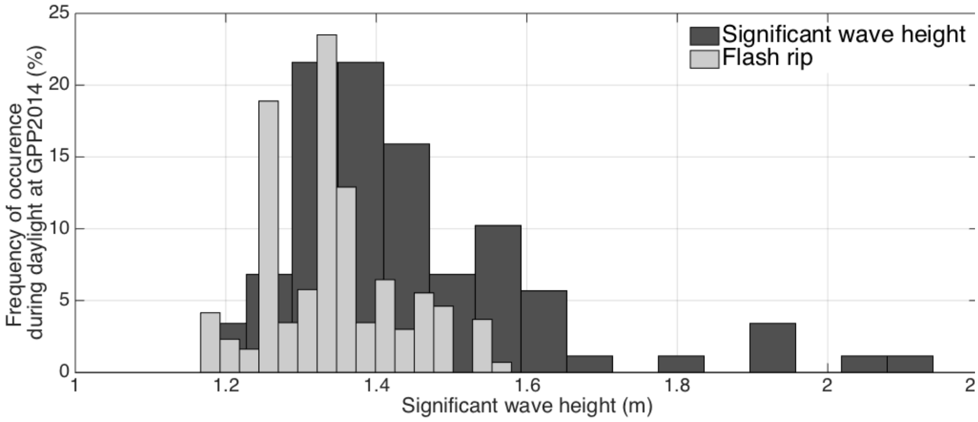

Figure 9: Frequency (%) of Flash-rip occurrence vs. Significant wave height.

Flash rip activity was maximized for approximately shore-normal (< 5°) wave incidence, with a SW prevalence of waves coming from South Atlantic (Figure 10).
This result is still proven by the decreasing trend of the flash rip-currents' lifetime according to the incidence, presented on Figure 10. The lifetime of flash rip-currents is low for very oblique waves. This is perhaps due to the increase in intensity of the longshore current according to the high incidence. Thus an intense longshore current would inhibit the generation of the flash-rip currents or at least they would dissipate faster the head of the rip.

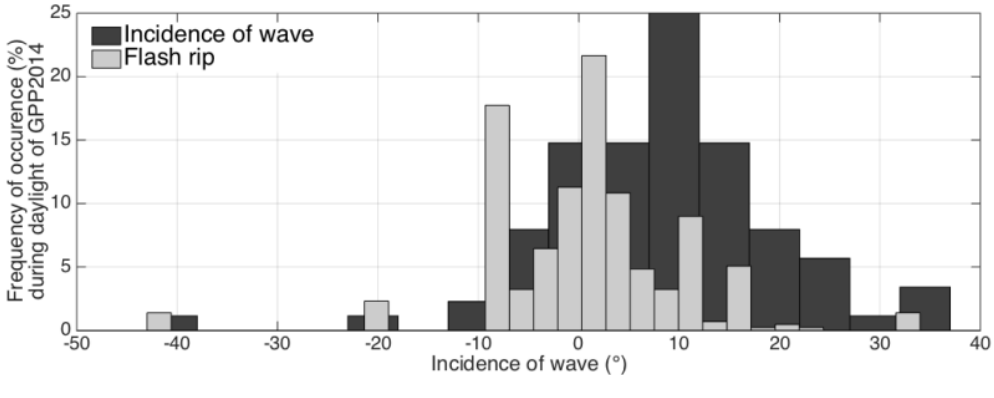

Figure 10: Frequency (%) of Flash-rip occurrence vs. Incidence of wave.

According to the rip current type classification developed in Castelle et al. (2016), this suggests that these hydrodynamically-controlled rips were driven by short-scale vorticity evolving freely as migrating surf-zone eddies (Feddersen, 2014) rather than driven by shear instabilities of the longshore current.

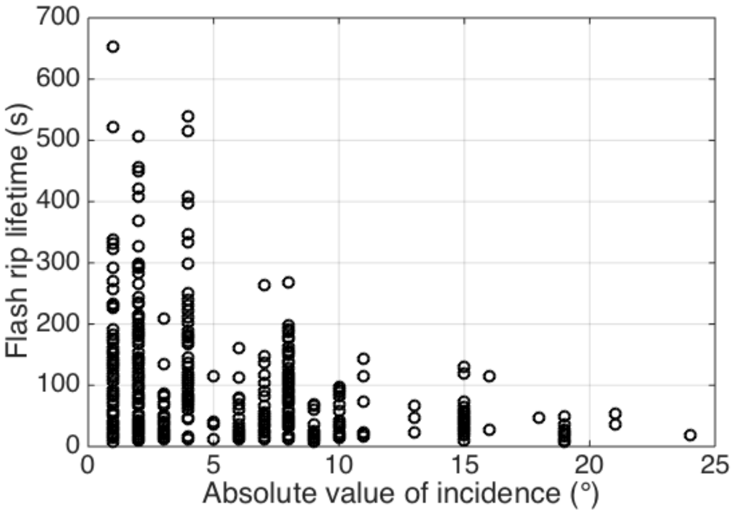

Figure 10: Flash-rip lifetime vs. Absolute value of incidence.

Figure 12 shows the impact of directional spreading on the longshore drift of the rip head and on the rip lifetime. These two rip caracterictics are increased with increasing spreading. On the contrary, the cross-shore extension is not shown to increase.

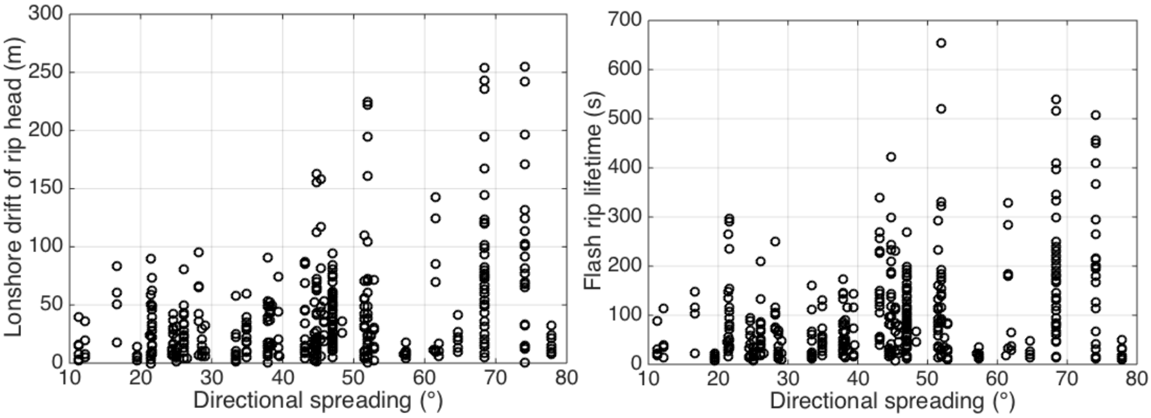

Figure 12: Impact of directional spreading on: *Left* Longshore drift of rip head and *Right* Flash rip lifetime

4. Limitations of Methods

The reflection of sunlight on the surface of the water is the principal difficulty to obtain a good contrast between the surface color in the turbidity flow generated in the rip and outside, making detection almost impossible. Certain atmospheric conditions such as the dew on the lens of camera and fog affect the quality of the primary images. Wind conditions can also influence the signal of the Flash-rip on the images with a state of stormy sea making the surf zone more disordered. Finally, visual verification of each flash rip-current makes this semi-automatic method very effective for detection but time-consuming for the obtention of flash-rip characteristics.

5. Conclusions

This study deals with generation mechanisms of flash rip-currents. The method used is the quantification of flash-rip via video images, according to a semi-automatic detection method based on color identification. 434 events of rip-currents were counted over one short period of seven days (57 hours of video processed). With mean lifetime around two minutes, cross-shore extension between 50 and 90 m and more flash rip activity at low tide under shore-normal wave incidence, our results are in agreement with the literature (Feddersen, 2014; Castelle et al., 2016). 65% of the total rips were observed to migrate alongshore with a velocity between 0.2 and 0.6 m/s (with a mean value of 0.45 m/s). Considering the short period of the study, the results are not representative of the range of conditions that may be expected. However, this study still shows the large amount of flash-rip occurring at Grand-Popo beach on 400 m of coastline. They represent a considerable hazard for the local population and further investigations need to be carried out to be able to predict the low-frequency modulation of these strong offshore currents. It would be very interesting to extend this analysis of the flash-rip characteristics over a whole year in order to consider the entire spectrum of conditions. For the moment, a more reliable statistics study is currently conducted on the dataset. The impact of the width of the spectrum is also investigated.

Acknowledgements

Grand Popo exp. funded by French INSU/CNRS EC2CO-LEFE/IRD, UNESCO co-chair ICPMA and IRHOB. We are greatly indebted to the naval services of Benin at Grand Popo for their logistic support during the field experiment and for allowing the installation of the permanent video system on the semaphore. This research has also received support from French grants through ANR (COASTVAR: ANR-14-ASTR-0019).

References

Birrien F., Castelle B., Dailloux D., Marieu V., Rihouey D., and Price T.D., 2013. Video observation of mega-cusp evolution along a highenergy engineered sandby beach. Plymouth, England : *Journal of Coastal Research*, Special Issue No. 65. *Proceedings 12th International Coastal Symposium*. pp. pp. 1727-1732.

Bowen A.J., Inman D.L., 1969. Rip currents : 2. Laboratory and field observations. *J. Geophys. Res*. 74, pp. p. 5479–5490.

Brander R.W., 1999. Field observations on the morphodynamic evolution of low wave energy rip current system. *Mar. Geol*. 157, pp. p.199–217.

Castelle B., Almar R., Dorel M., Lefebvre J-P., Sénéchal N., Anthony E. J., Laibi R., Chuchla R., du Penhoat Y., 2013, Rip currents and circulation on a high-energy low-tide-terraced beach (Grand Popo, Benin, West Africa), *Journal of Coastal Research*, Special Issue No. 66 (1-6).

Castelle B., Scott S., Brander R.W., McCarroll R.J., 2016. Rip current types, circulation and hazard, *Earth-Science Reviews*, 163, 1-21.

Cooke D.O., 1970. The occurrence and geologic work of rip currents off southern California. *Mar. Geol*. 9, pp. 173–186.

Feddersen F., 2014. The generation of surfzone eddies in a strong alongshore current. *J. Phys. Oceanog*., 44 : 600-617.

Inman D., Tait R., Nordstrom C., 1971. Mixing in the surf zone, *J. Geophys.Res*. 76 (C15) , pp. p.3493–3514.

Komar P.D., 1971. Nearshore cell circulation of the formation of giant cusps. *Geol. Soc. Amer. Bull*. 82, pp. 2643–2650.

Laibi, R., Anthony, E.J., Almar, R., Castelle, B., Sénéchal, N, Kestenare, E., 2013. Longshore drift cell development on the human-impacted Bight of Benin sand barrier coast, West Africa. *Journal of Coastal Research*, Special Issue No. 66.

Longuet-Higgins M.S., Stewart R.W., 1964. Radiation stress in water waves, a physical discussion with applications. *Deep-Sea Res*. 11 (4), pp. p.529–563.

MacMahan J., Thornton E.B., Stanton T.P., Reniers A.J.H.M., (2005). RIPEX—rip currents on a shore-connected shoal beach. *Mar. Geol*. 218, pp. p.113– 134.

Murray T., Cartwright N., Tomlinson R., 2013, Video-imaging of transient rip currents on the Gold Coast open beaches, *Journal of Coastal Research*, Special Issue No. 65, 1809-1814.

Peden, M.M. and McGee, K., 2003. The epidemiology of drowning worldwide. *Injury Control and Safety Promotion*, 10, 195-199.

Rafael Almar, cours: Processus hydro-sédimentaires littoraux. *rafael.almar@ird.fr*.

Shanks A.L., Morgan S.G., MacMahan J.H., 2010. Surf zone physical and morphological regime as determinants of temporal and spatial variation in larval recruitent. *Journal of Experimental Marine Biology and Ecology*, 392, pp. 140-150.

Short A., 1992. Beach systems of the central Netherlands coast : processes,morphology and structural impacts in a storm driven multi-bar system. *Mar. Geol*. 107, pp. p.103–137.

Short A.D., 1999. Handbook of Beach and Shoreface Morphodynamics. *John Willey and Sons*, p. p. 379.

Thornton E.B., MacMahan J.H., and Sallenger Jr. A.H., 2007. Ripcurrents, mega-cusps, and eroding dunes. *Marine Geology*, 240, pp. p.151-167.

World Health Organization, 2010. Drowning Fact Sheet 347. Available at http://www.who.int/mediacentre/factsheets/fs347/en/

Wright, L.D. and Short, A.D., 1984. Morphodynamics variability of surf zones and beaches: a synthesis. *Marine Geology*, 70: 251-285.